THE JOURNAL OF BIOLOGICAL CHEMISTRY VOL. 282, NO. 39, pp. 28385–28394, September 28, 2007
Printed in the U.S.A.

Modulation of Apolipoprotein A-IV Lipid Binding by an Interaction between the N and C Termini*

Received for publication, May 16, 2007, and in revised form, August 8, 2007 Published, JBC Papers in Press, August 8, 2007, DOI 10.1074/jbc.M704070200

Matthew R. Tubb[‡], **R. A. Gangani D. Silva**[‡], **Kevin J. Pearson**[§], **Patrick Tso**[‡], **Min Liu**[‡], **and W. Sean Davidson**[‡1]

From the [‡]*Department of Pathology and Laboratory Medicine, University of Cincinnati, Cincinnati, Ohio 45237 and the* [§]*Laboratory of Experimental Gerontology, NIA, National Institutes of Health, Baltimore, Maryland 21224*

Apolipoprotein A-IV (apoA-IV) is a 376-amino acid exchangeable apolipoprotein made in the small intestine of humans. Although it has many proposed roles in vascular disease, satiety, and chylomicron metabolism, there is no known structural basis for these functions. The ability to associate with lipids may be a key step in apoA-IV functionality. We recently identified a single amino acid, Phe^{334}, which seems to inhibit the lipid binding capability of apoA-IV. We also found that an intact N terminus was necessary for increased lipid binding of Phe^{334} mutants. Here, we identify Trp^{12} and Phe^{15} as the N-terminal amino acids required for the fast lipid binding seen with the F334A mutant. Furthermore, we found that individual disruption of putative amphipathic α-helices 3–11 had little effect on lipid binding, suggesting that the N terminus of apoA-IV may be the operational site for initial lipid binding. We also provide three independent pieces of experimental evidence supporting a direct intramolecular interaction between sequences near amino acids 12/15 and 334. This interaction could represent a unique "switch" mechanism by which apoA-IV changes lipid avidity *in vivo*.

Apolipoprotein A-IV (apoA-IV)[2] is a 46-kDa protein produced almost exclusively in the small intestine in humans (1, 2). Although it does not have a single, universally recognized function, apoA-IV has been proposed to play many roles in lipid metabolism. Perhaps the best studied are its roles in chylomicron assembly and secretion. ApoA-IV is secreted from enterocytes as part of triglyceride-rich chylomicrons (1), and its synthesis is increased dramatically upon consumption of a lipid-rich meal (1, 2). ApoA-IV knock-out mice, under unstressed conditions, exhibit normal lipid absorption (3). However, when apoA-IV release from the endoplasmic reticulum is genetically disrupted, apoB and lipoprotein secretion is inhibited (4). On the other hand, overexpression of human apoA-IV in porcine intestinal cells enhances basolateral lipid secretion via production of larger chylomicron-like particles (5). In addition, certain naturally occurring polymorphisms of apoA-IV result in altered chylomicron clearance after the particles have reached the circulation (6). These data point to an important role for apoA-IV in chylomicron metabolism especially during high fat meals (*e.g.* breast milk).

Given its likely role in triglyceride-rich lipoprotein metabolism, it is perhaps not surprising that genetic manipulation of apoA-IV results in interesting phenotypes with respect to plasma lipids and atherosclerosis. ApoA-IV knock-out mice have decreased high density lipoprotein levels (3). Transgenic overexpression of human or mouse apoA-IV results in a protection from atherosclerosis in mice fed a high fat diet or coupled with the apoE knock-out background (7–9). Multiple studies in humans have observed reduced plasma apoA-IV levels in patients with cardiovascular disease (10–13). Taken together, the evidence suggests that apoA-IV can be protective against atherosclerosis, and its mechanism of action warrants further study.

Human apoA-IV consists of 376 amino acids, making it the largest of the exchangeable apolipoproteins. Like other apolipoproteins in this class, apoA-IV has several 22-mer amino acid repeats predicted to form amphipathic α-helices. These helices are widely considered to be operational for lipid binding and, therefore, for the functionality of these proteins. In the closely related protein apoA-I, amphipathic helix 1 and, particularly, helix 10 have been identified as the initial lipid binding regions (14). It is believed that the two ends of apoA-I bind first to a lipid surface, followed by a cooperative binding of the rest of the helical segments. Furthermore, disruption of apoA-I helix 10 markedly reduces its ability to promote cholesterol efflux from cells via the ATP binding cassette transporter A1, a critical process for the maintenance of plasma high density lipoprotein levels (15).

During chylomicron lipolysis, apoA-IV rapidly leaves the particle surface and circulates either lipid-free or bound to high density lipoprotein lipid particles (1). There is much debate about the ratio of lipid-free *versus* lipid-bound apoA-IV in plasma; different groups have come to drastically different conclusions, probably due to differences in separation techniques (11). Still, many studies show that a significant fraction of apoA-IV circulates lipid-free in plasma (~30–77%) (1, 16, 17). It is there-

* This work was supported by National Institutes of Health Grants HL67093 and HL82734 (to W. S. D.), two predoctoral fellowships from the Ohio Valley Affiliate of the American Heart Association (to M. R. T. and K. J. P.), and a University of Cincinnati graduate research fellowship (to M. R. T.). The costs of publication of this article were defrayed in part by the payment of page charges. This article must therefore be hereby marked "*advertisement*" in accordance with 18 U.S.C. Section 1734 solely to indicate this fact.

[1] To whom correspondence should be addressed: Dept. of Pathology and Laboratory Medicine, University of Cincinnati, 2120 Galbraith Rd., Cincinnati, OH 45237-0507. Tel.: 513-558-3707; Fax: 513-558-1312; E-mail: Sean.Davidson@UC.edu.

[2] The abbreviations used are: apo, apolipoprotein; DMPC, 1,2-dimyristoyl-*sn*-glycero-3-phosphatidylcholine; PAGGE, polyacrylamide gradient gel electrophoresis; BS^3, (bis)sulfosuccinimidyl suberate; CPM, 7-diethylamino-3-(4′-maleimidylphenyl)-4-methylcoumarin; MS, mass spectrometry; FRET, fluorescence resonance energy transfer; POPC, 1-palmitoyl 2-oleoyl phosphatidylcholine; WT, wild type; ANS, 1-Anilinonaphthalene-8-sulfonic acid; aa, amino acids; STB, standard Tris buffer; DTT, dithiothreitol; MLV, multilamellar vesicle; SUV, small unilamellar POPC vesicle.

fore possible that different functions are carried out by apoA-IV depending on its lipidation state. It follows that a detailed understanding of the apoA-IV lipid binding mechanism will be a key piece of information for understanding apoA-IV function.

Given the apparent evolutionary relationship between apoA-I and apoA-IV, we hypothesized that, like apoA-I, the apoA-IV C terminus should contain helical regions that are crucial for lipid binding. What we discovered was the exact opposite; when the C-terminal 44 amino acids were removed from apoA-IV, the protein actually increased its lipid binding efficiency (18). We then undertook studies to locate particular regions within the protein that may interact to modulate lipid association. We found that the mutation of either phenylalanine 334 or 335 to alanine drastically increased the rate at which apoA-IV is able to reorganize 1,2-dimyristoyl-*sn*-glycero-3-phosphatidylcholine (DMPC) liposomes. However, if amino acids 11–20 were deleted, the mutant reversed to the slow lipid binding of wild type apoA-IV (19). In the current work, we have determined the exact residues present in the N terminus that are responsible for reversion to the slow lipid-binding phenotype. In addition, we have gathered evidence that indicates that these residues participate in an intramolecular interaction with a C-terminal domain of apoA-IV and that this interaction modulates its lipid interaction.

EXPERIMENTAL PROCEDURES

Materials—Primer synthesis was performed by the University of Cincinnati DNA Core (Cincinnati, OH) or IDT (Coralville, IA). DNA sequencing was performed at the Cincinnati Children's Hospital Research Foundation DNA Core. IgA protease was purchased from MoBiTec (Germany). BL-21 (DE3) *Escherichia coli* were from Protein Express (Cincinnati, OH). Isopropyl-β-D-thiogalactoside was purchased from Fisher (Hampton, NH). His-bind resin was purchased from Novagen (Madison, WI). DMPC was from Avanti Polar Lipids (Birmingham, AL). 1-Anilinonaphthalene-8-sulfonic acid (ANS) and tris-(2-carboxyethyl)phosphine hydrochloride were purchased from Molecular Probes/Invitrogen. Bis[sulfosuccinimidyl] suberate (BS^3) was from Pierce, and sequencing grade trypsin was from Promega. All chemical reagents were of the highest quality available. "WT" represents wild type recombinant human apoA-IV-1 (Thr^{347}/Gln^{360}) (20) unless otherwise specified.

Site-directed Mutagenesis—Deletion and point mutants of human apoA-IV were created by site-directed mutagenesis as described previously (18, 19) in the bacterial expression vector, pET30 (Novagen). Complete DNA sequences of positively screening clones were verified by sequencing the entire cDNA. N-terminal deletion and point mutant design were based on previous studies narrowing down the region important for modulating lipid binding to within aa 11–20 (19). The design of helical disruption mutants was based on helical wheel projections (Antheprot) of the 13 helices predicted by Segrest *et al.* (21). Predicted apoA-IV helical aa were as follows: H1, aa 7–31; H2, aa 40–61; H3, aa 62–94; H4, aa 95–116; H5, aa 117–138; H6, aa 139–160; H7, aa 161–182; H8, aa 183–204; H9, aa 205–226; H10, aa 227–248; H11, aa 249–288; H12, aa 289–310; H13, aa 311–332. Because helices 1 and 2 and helices 12 and 13 were studied by truncation in our previous studies (18), we investigated only H3–H11. Our mutants involved changing a hydrophobic residue in the middle of the hydrophobic helical face to an aspartic acid on the background of the fast F334A mutant. The mutants generated on the fast background were as follows: H3, L71D; H4, I104D; H5, V126D; H6, L148D; H7, I170D; H8, I192D; H9, L214D; H10, I236D; H11, L258D.

Protein Production—Human apoA-IV WT and mutant proteins were expressed as described previously using the T7 promoter and isopropyl 1-thio-β-D-galactopyranoside induction (18). In general, 600 ml of LB culture yielded 30–40 mg of uncut protein (>95% pure). Adequate expression was verified by SDS-PAGGE comparing cell lysate from induced and non-induced cultures. Cell pellets were solubilized in the presence of a protease inhibitor mixture (phenylmethylsulfonyl fluoride, leupeptin, pepstatin), disrupted by probe sonication, and protein was purified by affinity chromatography utilizing the vector's His tag and Ni^{2+} resin columns. The His tag was cleaved using the endoprotease, IgA protease, which cleaves the sequence PRPPTP, leaving an additional threonine and proline on the protein's N terminus. The cleaved tag was separated from cut protein using the nickel affinity column and collecting the flow-through containing >98% pure cut protein. Proteins were dialyzed into 10 mM ammonium bicarbonate, lyophilized, and stored at −20 °C in several-mg aliquots. Lyophilized proteins were reconstituted in standard Tris buffer (STB; 150 mM NaCl, 10 mM Tris-HCl, pH 8.0, 1 mM EDTA, 0.02% sodium azide) plus 3 M guanidine and dialyzed into STB before use. Protein degradation was monitored by SDS-PAGGE, and proteins were not used if significant degradation was observed. Before each experiment, protein concentration was determined in a single Markwell-Lowry protein assay (22). For the cysteine mutants, serine 16 and/or 336 were replaced with a cysteine by site-directed mutagenesis as described above. Cysteine mutants were purified using the standard nickel column method. Purification by ammonium sulfate precipitation to avoid cysteine exposure to nickel did not affect labeling efficiency of the cysteine. For the disulfide linkage experiments (Fig. 7), 2Cys F334A protein was refolded by dialysis from 3 M guanidine into STB in the presence of 5 mM DTT. Only after the protein was in its native conformation in STB + 5 mM DTT was the DTT dialyzed out to allow for disulfide bond formation. Monomeric 2Cys F334A protein was isolated by tandem size exclusion chromatography with no DTT present, and isolated monomeric protein was identified by non-reducing SDS-PAGGE.

Lipid Binding Assays—The rate of lipid association was determined using the DMPC liposome clearance assay (23, 24). Briefly, DPMC multilamellar vesicles (MLVs) at 5 mg/ml were prepared in STB by brief probe sonication. MLVs and STB were mixed, so that once protein was added, the final DMPC concentration was 0.425 mg/ml. Protein was quickly added to the above mixture to a final 0.17 mg/ml protein concentration (2.5:1 DMPC/protein, w/w). Proteins for all experiments were in STB except for the experiment presented in Fig. 7, which was in STB with and without 5 mM DTT. Absorbance at 325 nm was measured in an Amersham Biosciences Ultraspec 4000 UV-visible spectrophotometer at 24.5 °C at 30-s intervals for 20

min. Samples were run in triplicate, and plots were normalized to the initial absorbance of the sample (OD_0). The clearance of the reaction is due to apoprotein binding to, and solubilization of, the MLVs to small discoidal lipoproteins that do not scatter light at 325 nm. The assay was carried out at 24.5 °C, the gel/liquid crystal transition temperature of DMPC, where an optimal number of lattice defects exist on the MLV surface. Each result was verified by at least one additional DMPC experiment on a separate day from an independent protein expression. The DMPC liposome clearance assay is a multistep reaction that involves binding to the lipid surface followed by an unknown reorganization step. Thus, this assay is not strictly a measure of lipid binding. However, it has been proposed that the initial binding steps are rate-limiting and that once a critical number of apoproteins bind to the lattice defects on the MLV surface, the rate of reorganization is similar for all proteins (24). To more specifically focus on the lipid binding step in isolation, we studied select mutants and WT apoA-IV using the biotin capture lipid affinity assay (25). Briefly, a constant mass of small unilamellar POPC vesicles (SUVs) containing small amounts of biotinylated lipid and fluorescently labeled lipid were mixed with increasing amounts of apolipoprotein in a microplate setup. After binding reached equilibrium, vesicle-bound protein was separated from unbound protein in a 96-well streptavidin column plate. K_d values and n values were calculated based on bound *versus* total loaded protein and total phospholipid content using a fluorescent protein assay and the fluorescent lipid. Unlike DMPC, POPC SUVs do not reorganize, allowing us to observe the binding event in isolation.

Spectroscopy—ANS, a probe that fluoresces only when in contact with hydrophobic surfaces (26), was reacted with WT, F334A or W12A/F15A/F334A and with WT human apoA-I for comparison at room temperature in STB. Briefly, proteins were diluted to 50 μg/ml (1.15 μM), and ANS was added in excess at 250 μM. ANS was excited at 395 nm in a Photon Technology International Quantamaster fluorescent spectrophotometer, and emission was scanned from 400 to 600 nm. Samples were run in triplicate, and curves were corrected for buffer emission. For circular dichroism studies, proteins were freshly dialyzed against 20 mM phosphate buffer (pH 7.4), and relative concentration was determined by the Markwell-Lowry method. Proteins were then diluted to 100 μg/ml, and spectra were collected on a Jasco J-715 spectropolarimeter in a 1-mm cell as an average of three scans. The scans were from 260 to 190 nm at 50 nm/min with a 0.5-nm step size and 0.5-s response. Bandwidth was set to 1 mm, and slit width was 500 μm. To confirm the accuracy of dilution, protein concentration was verified by A_{280} on the diluted wild type apoA-IV sample, and mean residual ellipticity was calculated based on this value for all three protein samples. Mean residual ellipticity was calculated as described by Woody (27) using 115.3 as the mean residual weight for apoA-IV. Fractional helical content was calculated using the formula of Chen *et al.* (28) and the mean residual ellipticity at 222 nm. Each experiment was repeated three times with a similar pattern observed consistently.

Protein Labeling and Fluorescence Resonance Energy Transfer (FRET) Analysis—S336C was reduced in excess tris-(2-carboxyethyl)phosphine hydrochloride and freshly dialyzed against three changes of STB overnight. Results shown are from uncut protein still containing the His tag; however, similar experiments were conducted on cut protein, yielding comparable results. The pH was set to 6.5–7 in 1 ml of protein at 10 mg/ml for optimal cysteine specificity of the probe. While protected from light, CPM probe was reconstituted in Me_2SO and added dropwise to the protein to a final mol/mol ratio of 2:1 (probe/protein). The reaction was carried out in the dark, overnight on a shaker at room temperature. WT apoA-IV was also labeled to monitor for nonspecific labeling. An equal volume of Me_2SO was added to an additional set of proteins for the unlabeled (no acceptor) samples. Labeled and mock-labeled samples were dialyzed against three changes of STB to remove excess unreacted probe. Size exclusion chromatography was used for other sample preparations with negligible difference in results. Labeled or mock-labeled proteins were diluted in STB to a final concentration of 100 μg/ml for fluorescent measurements in order to reduce intermolecular interactions. FRET to the CPM acceptor probe was monitored by exciting the single tryptophan donor at 295 nm to minimize tyrosine excitation, and emission was scanned from 300 to 550 nm. Data were collected using a quartz cuvette in a Photon Technology International Quantamaster fluorescent spectrometer in photon counting mode at room temperature. Excitation and emission band passes were 3.0 nm. Buffer blanks were subtracted from each of the sample curves. Distance between donor and acceptor was calculated using the formula,

$$E \times 1/f_A = R_o^6/(R_o^6 + R^6) \quad \text{(Eq. 1)}$$

where $E = 1 - I_{DA}/I_D$, and f_A is the fractional labeling efficiency of the protein with the acceptor probe. I_{DA} is the donor emission intensity in the presence of the acceptor, and I_D is the intensity in the absence of the acceptor. R_o is the Forster radius for the donor-acceptor pair used, Trp-CPM, and was set to 29 Å, which has been reported (29, 30).

Cross-linking Analysis—Lipid-free WT apoA-IV was prepared for structural analysis in much the same way as by Silva *et al.* (31). Briefly, WT apoA-IV (~5 mg/ml) was dialyzed into phosphate-buffered saline (pH 7.8) and cross-linked with the homobifunctional cross-linker BS^3 at a final BS^3/protein molar ratio of 10:1 and final protein concentration of 1–3 mg/ml. BS^3 has the ability to react with δ-amino groups of lysine residues and the N-terminal primary amino group of a protein. During this reaction, BS^3 bridges two such nearby reactive groups within its spacer arm length of 11.4 Å. BS^3 was handled with minimal exposure to air to minimize hydrolysis. The cross-linker was suspended in phosphate-buffered saline and added to the protein within 1 min. The reaction was carried out for 18 h at 4 °C with gentle vortexing every 15 min for the first 1 h. At this point, the reaction was quenched with 100 mM Tris-HCl (pH 8.0), and the cross-linked protein was concentrated to a final volume of 300 μl. The sample was then applied to a tandem size exclusion column setup (Superose 6/Superdex 200) equilibrated in STB with 3 M guanidine, and monomer was separated from cross-linked dimer. Monomeric apoA-IV was exhaustively digested with sequencing grade trypsin (5% (w/w)) overnight, and 75–100-μg aliquots of trypsinized cross-linked

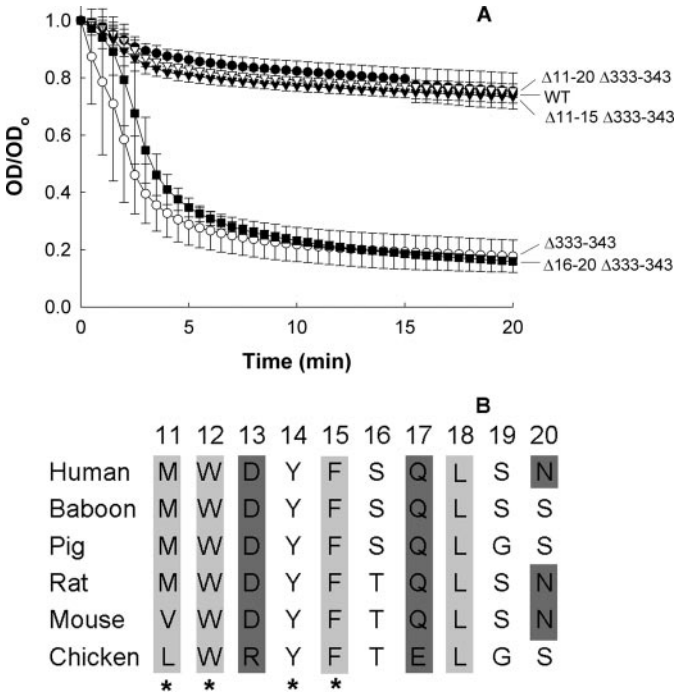

FIGURE 1. **Lipid association of N-terminal deletion mutants of apoA-IV.** *A*, DMPC liposome clearance assay of N-terminal deletion mutants of apoA-IV on fast mutant background. DMPC liposomes were mixed with protein samples, 2.5:1 (w/w), and OD was monitored over 20 min. Removal of amino acids 11–15 reversed the fast lipid-binding Δ333–343 mutant to WT-like lipid binding. Wild type apoA-IV is represented by *closed circles*. All *traces* represent means of triplicates during the same experiment. Results shown represent one experiment of multiple experiments performed on each mutant, each producing similar findings. *B*, sequence homology among species of apoA-IV residues 11–20 (hydrophobic residues in *lightly shaded boxes*, polar or charged groups in *dark shaded boxes*, and intermediate residues left *blank*). The *asterisks* represent residues mutated to alanine in subsequent studies.

monomeric apoA-IV were lyophilized and stored at −20 °C until use. Digested protein samples were analyzed on an Applied Biosystems Q-Star XL mass spectrometer equipped with an online Agilent 1100 capillary high performance liquid chromatograph as described previously (31, 32). The cross-linked peptide pair described in this paper (1–25 × 333–343) was identified by mass and by tandem mass spectrometry. Its identity was confirmed in three of three mass spectrometer runs for which MS/MS data were available.

Statistics—Mean and sample S.D. were determined for all applicable sample sets performed in triplicate. Any difference between two sample population means was determined using Student's *t* test, and *p* values were calculated from the *t* value and degrees of freedom. *p* values less than or equal to 0.05 were considered statistically significant. All lipid binding experiments were performed at least two times independently, yielding similar results. The figures show one such experiment. Absolute *k* values depend highly on exact experimental temperature and can therefore vary from experiment to experiment. Therefore, every experiment includes a wild type control and a fast mutant control so that the rate constant comparisons can be made within that experiment.

RESULTS

Identification of N-terminal Residues That Modulate ApoA-IV Lipid Binding—Fig. 1 shows that WT apoA-IV was relatively ineffective at clearing DMPC liposomes compared with the Δ333–343 mutant, as shown previously (19). However, simultaneous deletion of residues 11–20 in the Δ333–343 background reverted this fast mutant to the slow phenotype of the WT. Thus, certain amino acids within this N-terminal sequence appeared to be critical for the lipid binding of apoA-IV. To identify the residues involved, we created two smaller deletion mutants of 5 aa to divide the region in half. Δ16–20/Δ333–343 apoA-IV retained the fast lipid binding phenotype (Fig. 1). By contrast, deleting residues 11–15 blunted the lipid binding. Rate constants calculated for the first 5 min of the reaction are listed in Table 1. Fig. 1*B* shows that the region 11–15 contains three positions occupied by hydrophobic amino acids that are conserved across species. We next used site-directed mutagenesis to change each residue in this region to alanine on the Δ333–343 background. Changing Met[11] and Tyr[14] did not affect the lipid-solubilizing phenotype (Table 2). However, the mutants W12A and F15A showed a statistically significant slowing effect on Δ333–343 lipid association (Fig. 2*A*, Table 2). Combining these two mutations, W12A/F15A/Δ333–343, reversed the fast Δ333–343 phenotype to nearly wild type levels (Table 2). Fig. 2*B* shows that mutation of these two residues had an identical effect on the background of the point mutant F334A. It is also clear that apoA-IV Δ333–343 behaved identically to apoA-IV F334A as previously described (19).

The DMPC assay used above is an index of a given protein's ability to bind to and reorganize lipid. To get an idea of the lipid binding characteristics only, we used the biotin capture lipid affinity assay, which measures protein association with a stable POPC SUV without further rearrangement (25). Wild type apoA-IV exhibited a K_d of 0.627 μM (Fig. 3, Table 3). Surprisingly, both F334A and W12A/F15A/F334A exhibited a slightly but significantly lower K_d and an increase in overall capacity for binding the vesicles compared with WT.

TABLE 1
DMPC clearance rate constants for N-terminal deletion mutants

	k^a	*p* (*versus* WT)[b]	*p* (*versus* Δ333–343)[b]
WT	0.03 ± 0.01		0.007
Δ333–343	0.28 ± 0.08	0.007	
Δ11–20 Δ333–343	0.05 ± 0.01	0.110	0.009
Δ11–15 Δ333–343	0.04 ± 0.01	0.390	0.008
Δ16–20 Δ333–343	0.20 ± 0.04	0.002	0.230

[a] *k* is the rate constant derived from the first 5 min of the DMPC clearance assay ± S.D.
[b] *p* values calculated from the mean and S.D. using Student's *t* test.

TABLE 2
DMPC clearance rate constants for N-terminal point mutants

	k^a	*p* (*versus* WT)[b]	*p* (*versus* Δ333–343)[b]
WT	0.069 ± 0.005		<0.0001
Δ333–343	0.44 ± 0.04	<0.0001	
M11A Δ333–343	0.38 ± 0.06	0.001	0.24
W12A Δ333–343	0.23 ± 0.03	0.001	0.0011
Y14A Δ333–343	0.38 ± 0.07	0.002	0.24
F15A Δ333–343	0.27 ± 0.03	0.0003	0.0012
W12A/F15A/Δ333–343	0.12 ± 0.02	0.02	0.0002
F334A	0.38 ± 0.02	0.0001	
W12A/F15A/F334A	0.11 ± 0.03	0.06	0.0001[c]

[a] *k* is the rate constant derived from the first 5 min of the DMPC clearance assay, shown ± S.D.
[b] *p* values calculated from the mean and S.D. using Student's *t* test.
[c] *p* value is *versus* F334A fast mutant, not Δ333–343.

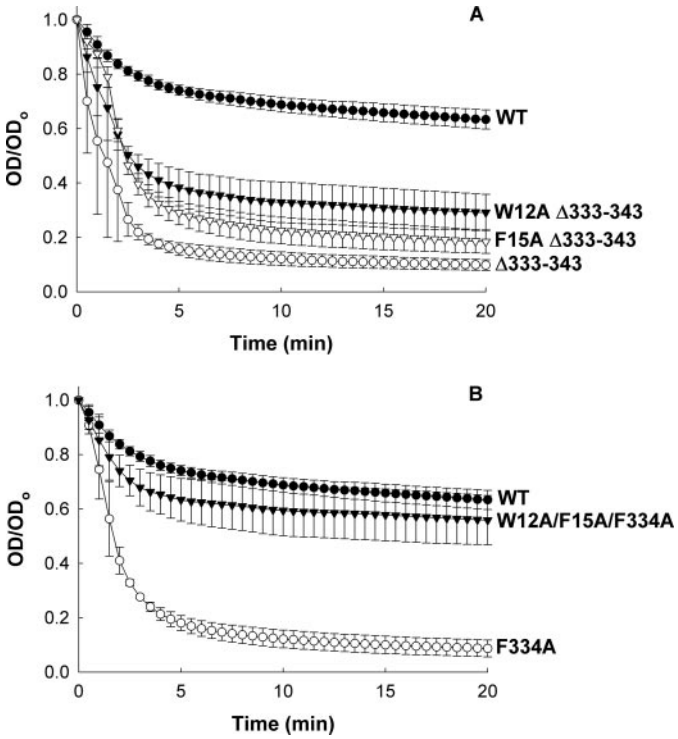

FIGURE 2. **Lipid association of N-terminal point mutants of apoA-IV.** DMPC liposomes were mixed with protein samples, 2.5:1 (w/w), and OD was monitored over 20 min. *A*, two mutants (W12A and F15A) had an intermediate effect on reversal toward WT. *B*, combination of the two mutations shown in *A* results in complete reversal of the F334A fast point mutant to WT lipid binding. All *traces* represent means of triplicates during the same experiment. Results shown represent one experiment of multiple experiments performed on each mutant, each producing similar findings.

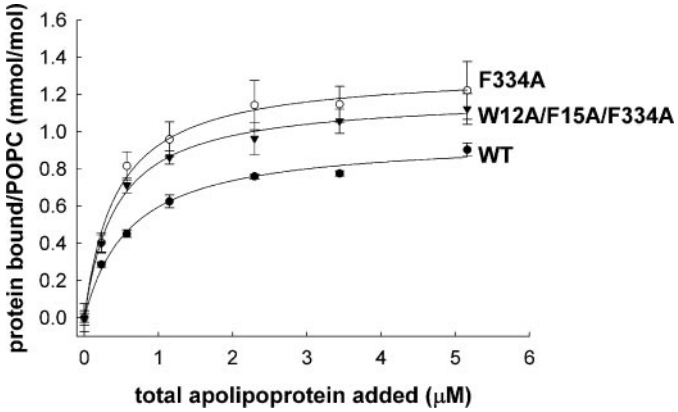

FIGURE 3. **Lipid affinity of N- and C-terminal point mutants of apoA-IV.** POPC SUVs were incubated with various concentrations of protein sample. Lipid-bound protein was isolated using a microplate streptavidin column setup; protein and lipid were quantified using fluorescence. *Closed circles*, WT; *open circles*, F334A; *closed triangles*, W12A/F15A/F334A. A biotin capture lipid affinity assay was performed multiple times in triplicate at room temperature. Data shown were derived from one such experiment.

Structural Characterization of the Mutants—To determine how the identified point mutations affect the overall structure of apoA-IV, we analyzed the exposure of hydrophobic residues to ANS, a molecule that fluoresces only when exposed to hydrophobic residues or lipid bilayers (26). Fig. 4 shows that ANS was minimally fluorescent when exposed to both WT and F334A. Mutation of the two N-terminal residues in W12A/F15A/F334A resulted in a 38% increase in fluorescence *versus* the

TABLE 3
BCLA assay data

	K_d[a]	p[b]	n[c]	p
	μM			
WT apoA-IV	0.63 ± 0.09		0.97 ± 0.04	
F334A	0.43 ± 0.04	0.03	1.3 ± 0.08	0.003
W12A/F15A/F334A	0.43 ± 0.01	0.02	1.2 ± 0.06	0.0004

[a] K_d ± S.D. is the dissociation constant calculated using the formula previously described.
[b] p values calculated from the mean and S.D. using Student's t test.
[c] n is the maximum number of binding sites present on the vesicles for apolipoprotein binding, shown ± S.D.

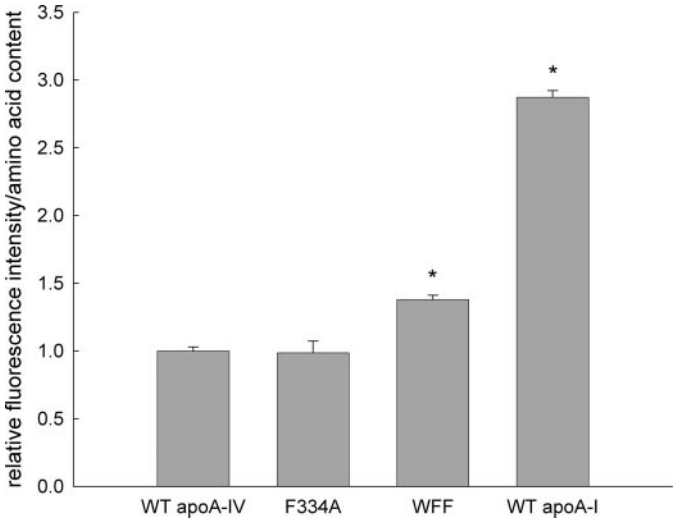

FIGURE 4. **Hydrophobic exposure of N- and C-terminal point mutants of apoA-IV.** ANS was added in excess at 250 mM to proteins at 50 μg/ml in standard Tris buffer. ANS was excited at 395 nm, and emission was scanned from 400 to 600 nm. The *bar graph* represents mean peak fluorescence intensity corrected for amino acid content of the recombinant proteins and relative to average peak WT apoA-IV fluorescence. The *WFF column* represents the W12A/F15A/F334A results. Samples were run in triplicate at room temperature. Significant difference ($p > 0.05$) compared with WT apoA-IV is indicated by an *asterisk*.

WT. By contrast, human WT apoA-I resulted in nearly triple the fluorescence of the WT apoA-IV. These data indicate that the F334A mutation does not significantly unfold the protein to expose more hydrophobic surface area, whereas further mutations in the N terminus do have a small effect. However, these changes are minimal compared with the hydrophobic exposure observed in apoA-I.

We utilized CD to estimate the secondary structure of the apoA-IV point mutants. CD measurements revealed that WT apoA-IV as well as both point mutants exhibited the classical pattern for a mainly α-helical protein with minima at 208 and 222 nm (Fig. 5). Consistent with the ANS data in Fig. 4, the spectra for WT and F334A were nearly superimposable. The calculated α-helicity for these proteins was 60 and 58%, respectively. Again, W12A/F15A/F334A was slightly different, with a lower helicity of 45%, consistent with the increased exposure of hydrophobic residues apparent in Fig. 4.

A Potential Interaction between the N- and C-terminal Sequences—We have previously speculated that the C-terminal sequence around Phe^{334} in apoA-IV may interact with an N-terminal site to modulate apoA-IV lipid affinity, perhaps to keep a helical bundle structure from opening up. Now that we

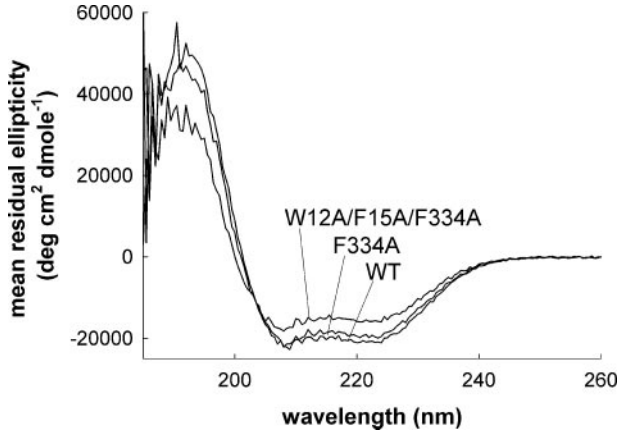

FIGURE 5. **Circular dichroism measurements of N- and C-terminal point mutants of apoA-IV.** Far UV spectra were obtained for wild type and mutant apoA-IV using a spectropolarimeter. Mean residual ellipticity was calculated as described under "Experimental Procedures."

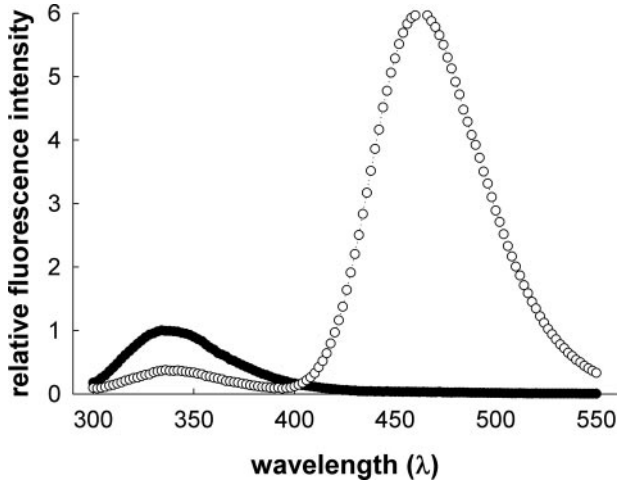

FIGURE 6. **Intramolecular fluorescence resonance energy transfer within apoA-IV.** Energy transfer between the endogenous Trp[12] donor and a CPM acceptor probe located on an introduced cysteine at position 336. *Black trace*, S336C apoA-IV without acceptor probe (CPM); *white trace*, S336C + CPM acceptor probe. FRET carried out at room temperature with protein at 100 μg/ml in STB. Tryptophan was excited at 295 nm. The addition of acceptor probe resulted in reduction in tryptophan emission (334 nm) and resultant acceptor emission at 462 nm due to energy transfer between the two probes. The *y* axis shows intensity relative to maximum Trp emission of unlabeled protein. Data shown represent one of three similar experiments conducted; all yielded comparable results.

have identified the exact residues modulating lipid binding in the N terminus, we set out to test this hypothesis. We first performed an intramolecular FRET experiment. We took advantage of the single tryptophan at position 12, which is involved in the modulation of lipid affinity (see Fig. 2), to serve as a FRET donor. The acceptor was a coumarin group substituted onto an introduced Cys residue at position 336. In the absence of acceptor probe, the tryptophan, excited at 295 nm, emitted fluorescence at a maximum of 334 nm (Fig. 6, *closed circles*) signifying that the tryptophan is in a hydrophobic environment (34). Upon the addition of the acceptor probe, energy transfer was observed as a 63% decrease in tryptophan fluorescence and prominent acceptor fluorescence at 462 nm (Fig. 6, *open circles*). Since the Forster radius (distance where energy transfer is 50% efficient) for the probe pair is 29–31 Å (29, 30), the magnitude of energy transfer supports a close spatial relationship between the two linearly distant regions. This experiment was also performed in STB with 3 M guanidine, and as expected, the acceptor probe fluorescence decreased substantially due to protein unfolding (data not shown).

As a second approach to study the potential interaction between these two sites, we constructed a double cysteine mutant of apoA-IV on the fast F334A background. Similar disulfide linkage studies in apoE and apolipophorin III have revealed information about how those proteins interact with lipid (35, 36). The Cys residues were substituted for neutral amino acids at position 336, near our identified C-terminal site, and at position 16, near the N-terminal site. If our interaction hypothesis is correct, we expected that a disulfide bond should form only if the two areas are near each other in the native conformation of lipid-free apoA-IV. We reasoned that formation of a disulfide should prevent conformational changes required for lipid binding and cause the mutant to lose its ability to solubilize DMPC liposomes. However, upon reduction of the disulfide, we expected that the mutant should recover its lipid solubilization characteristics. Fig. 7*A* shows that the double cysteine mutant, 2Cys F334A, was unable to rapidly associate with lipids, being similar to WT protein. However, upon reduction of the disulfide bond with 5 mM DTT, the double cysteine mutant exhibited significantly faster lipid binding (Fig. 7*A*, Table 4), approaching that of apoA-IV F334A alone. On the other hand, neither WT nor F334A lipid binding was significantly affected by the addition of DTT to the DMPC assay. In order to rule out potential intermolecular cross-linkage effects, we repeated the experiment with monomeric double cysteine mutant isolated from dimeric forms by size exclusion chromatography and achieved similar results (Fig. 7*B*). This suggests that the N and C termini of monomeric apoA-IV reside close enough to form an intramolecular disulfide bond that inhibits lipid binding. To further confirm an intramolecular disulfide bond, we analyzed similar samples by electrospray tandem mass spectrometry. Fig. 7*C* shows the mass spectrum of the disulfide-linked peptide pair of aa 1–25 (containing the Cys residue at position 16) and aa 333–341 (containing Cys at position 336) with a molecular mass of 3829.830 Da. The MS/MS fragmentation pattern from this ion unequivocally confirmed the presence of the disulfide linkage between these two sites in the native protein conformation.

As a third approach, cross-linking chemistry and mass spectrometry were used to determine if peptides from these two sites in WT protein could be linked with a homobifunctional cross-linking agent of a specified length. Lipid-free WT apoA-IV in solution was cross-linked with BS^3. Monomeric apoA-IV was separated from any oligomerized forms by gel filtration chromatography, exhaustively trypsinized, and analyzed by electrospray mass spectrometry. Among others (not shown), we identified the cross-linked peptide 1–25 × 333–343. As shown in Fig. 8, 17 possible MS/MS fragment peptide masses were identified for this cross-linked pair, unambiguously confirming its identity. These data suggest that the amino groups of the N-terminal Thr and residue 341 (Lys), the residues linked by BS^3, lie within 12 Å of each other in the native conformation of WT apoA-IV. The N-terminal Thr is actually

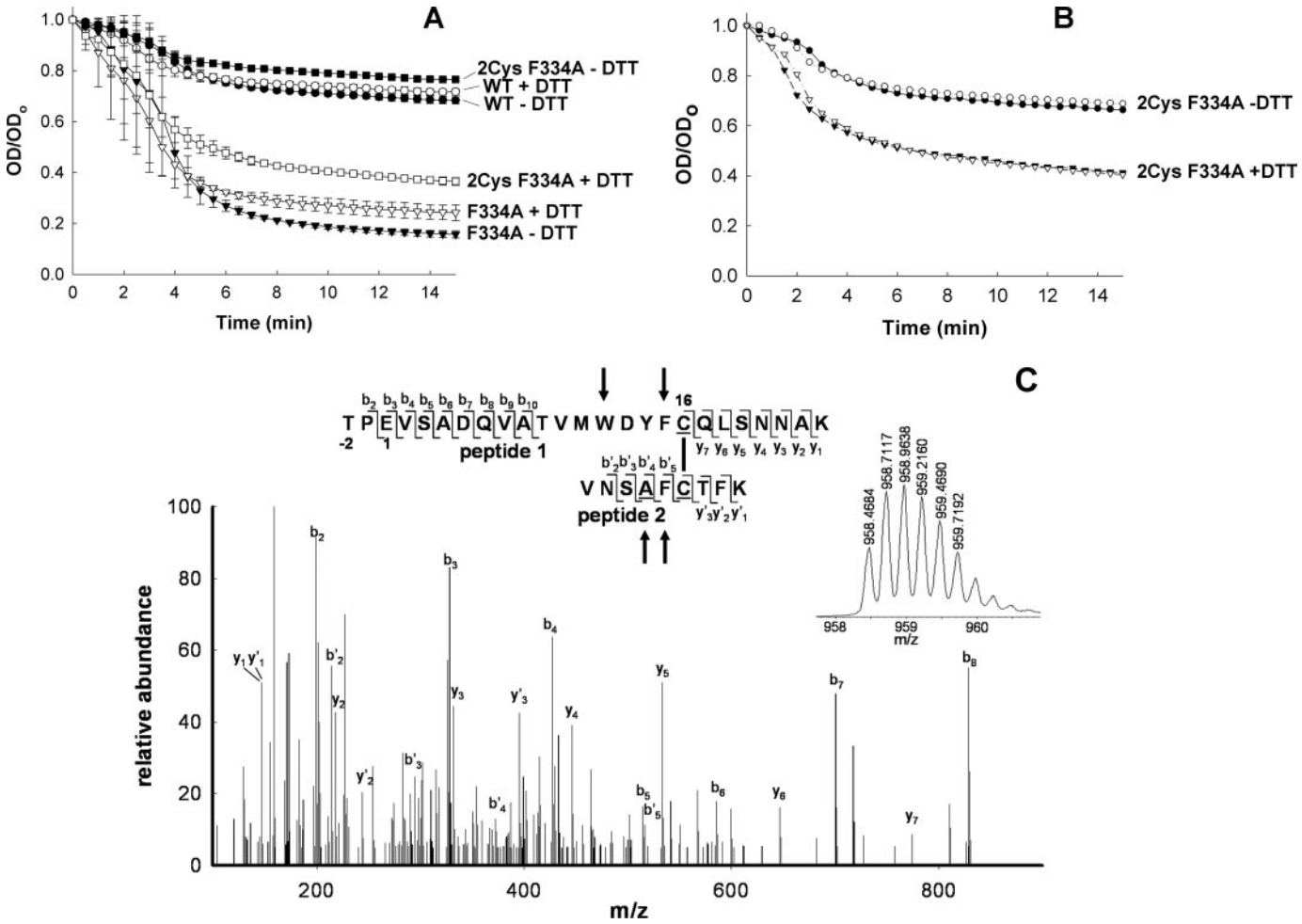

FIGURE 7. **Lipid association of a double cysteine mutant on the fast F334A apoA-IV background.** DMPC liposomes were mixed with protein samples, 2.5:1 (w/w), with or without 5 mM DTT, and OD was monitored over 15 min. *A*, cysteine oxidation attenuates lipid binding, and reduction with 5 mM DTT restores fast lipid binding; WT and F334A with or without DTT were run as controls. *B*, lipid binding of purified monomeric protein verifies the existence and importance of an intramolecular disulfide between residues 16 and 336; individual replicates are shown in lieu of mean and S.D. due to limited protein. *Circles*, monomeric protein under oxidizing conditions; *triangles*, the protein under reducing conditions (+5 mM DTT). *C*, mass spectrometric evidence for the internal disulfide linkage between residues 16 and 336. Monomeric 2Cys F334A apoA-IV protein was isolated by gel filtration chromatography under nonreducing conditions, and tryptic peptides were analyzed by mass spectrometry. The mass spectrum of the +4 ion of the disulfide-linked peptide 1–25 × 333–341 (M_r 3829.830) is shown in the *inset* with the MS/MS fragmentation pattern (b and y ions) shown below. Peptide 1 fragments b-9 and b-10 were also present but not shown due to their higher *m/z*. The amino acid sequence of the linked peptides are shown with those involved in the proposed N/C-terminal interaction indicated by the *arrows*. Mutated residues are *underlined*.

TABLE 4
DMPC clearance rate constants for double cysteine mutants

	5 mM DTT	K^a	p^b
WT	−	0.043 ± 0.01	0.46 (from 2Cys F334A$^-$)
2Cys F334A	−	0.036 ± 0.01	0.0082 (from 2Cys F334A$^+$) 0.46 (from WT$^-$)
2Cys F334A	+	0.13 ± 0.03	0.0082 (from 2Cys F334A$^-$) 0.13 (from F334A$^+$)
F334A	+	0.20 ± 0.05	0.13 (from 2Cys F334A$^+$)
2Cys F334A monomer	−	0.056	NA[c]
2Cys F334A monomer	+	0.14	NA

[a] k is the rate constant derived from the first 5 min of the DMPC clearance assay, shown ± S.D.
[b] p values calculated from the mean and S.D. using Student's t test.
[c] NA, not available because $n = 2$.

the first of two additional N-terminal amino acids left after cleavage of the His tag in our recombinant construct. Therefore, position 341 in the recombinant form corresponds to position 339 in the wild type apoA-IV molecule and is only five amino acids away from Phe[334]. Similarly, the N-terminal Thr is 13 and 16 amino acids away from Trp[12] and Phe[15], respectively, corresponding to 3–4 helical turns.

Scanning for a Lipid Binding Helix in ApoA-IV—In order to determine if additional helical segments within apoA-IV play a role in lipid binding, each of the predicted amphipathic helices of apoA-IV, from helix 3 to helix 11, was disrupted individually by insertion of a charged aspartic acid residue in the middle of the hydrophobic helical face in place of a strongly hydrophobic residue. This same mutation in helix 10 of apoA-I, known to be crucial for its lipid interactions (14), resulted in a drastic slowing effect in the DMPC assay (data not shown). ApoA-IV helices 1, 2, 12, and 13 were not studied, because previous deletion of these domains had no effect on lipid binding (18, 19). All mutants were generated on a background of the fast lipid binding mutant F334A. Fig. 9 shows that nearly all of the helical disruption mutants reorganized DMPC with similar kinetics as F334A itself, implying that those particular helices were not

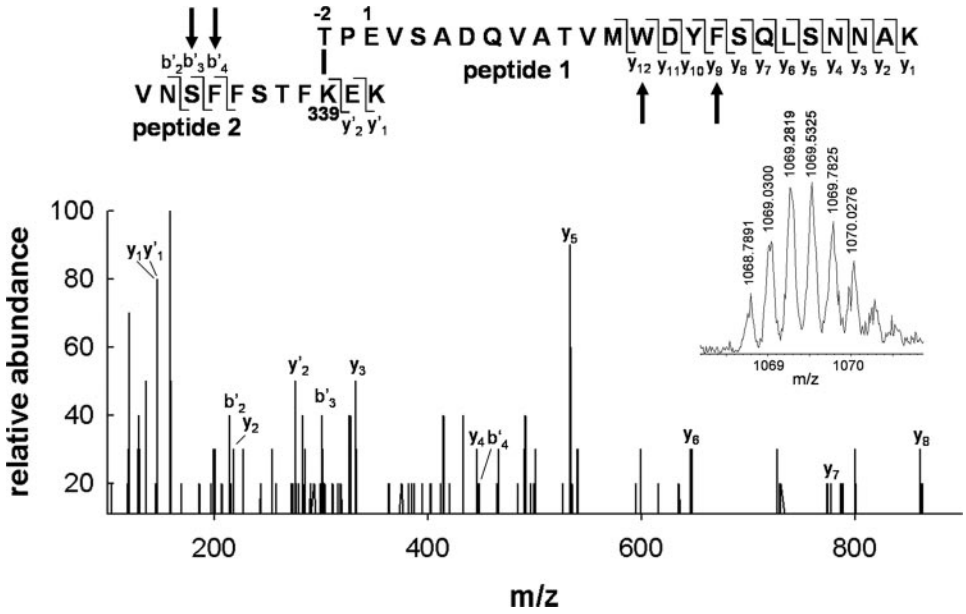

FIGURE 8. **MS/MS evidence for the intramolecular cross-link T-2-K339 between peptides 1–25 and 333–343 in the WT protein.** Proximal lysine residues in WT apoA-IV protein were cross-linked with BS^3, monomeric protein was isolated, and tryptic peptides were analyzed by mass spectrometry. MS/MS fragments (b and y ions) resulted from amide bond cleavage of the cross-linked peptide 1–25 × 333–343 (M_r 4271.1876). Cross-linked peptide shown (*top*) is represented using single-letter amino acid code. MS/MS peaks corresponding to fragments are shown (*bottom*). Peptide 1 fragments y-9 to y-12 were also present but not shown due to their higher *m/z*. Amino acids important in lipid binding assay and involved in proposed N/C-terminal interaction are indicated by the *arrows*. *Inset*, parent ion of 1–25 × 333–343 (+4 charge state).

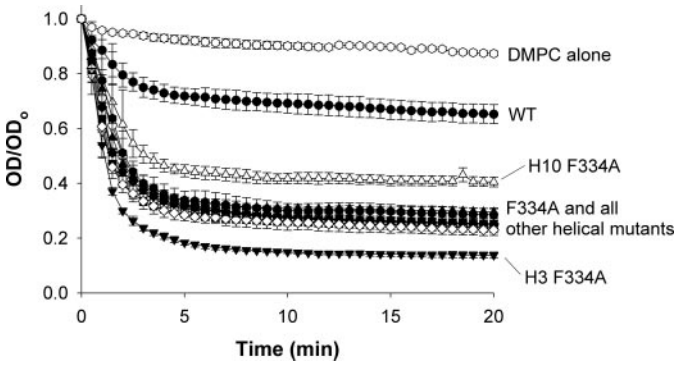

FIGURE 9. **Lipid association of helical disruption mutants on the fast F334A apoA-IV background.** DMPC liposomes were mixed with protein samples, 2.5:1 (w/w), and OD was monitored over 15 min. Disruption of helix 10 has a slight slowing effect on the fast lipid-binding apoA-IV mutant, whereas helix 3 disruption results in a slight further enhancement of lipid binding. All other helices tested (H4, H5, H6, H7, H8, H9, and H11) show no change in this assay from the F334A mutant. *Top trace*, DMPC lipid alone with no apolipoprotein added.

important for lipid binding. Disruption of helix 3 (H3 F334A) modestly but significantly increased the rate of lipid association beyond that of F334A, whereas disruption of helix 10 (H10 F334A) led to a slight decrease in lipid binding rate.

DISCUSSION

We have previously demonstrated that the mutation of a single Phe residue at position 334 or 335 can cause apoA-IV to bind to and reorganize lipids even more effectively than apoA-I (19). We also showed that the apoA-IV N terminus is required for the manifestation of this accelerated lipid binding phenotype. In the current study, we followed up on these observations and found the following. 1) The critical N-terminal residues mediating the increased lipid binding when residue 334 is disrupted are Trp^{12} and Phe^{15}. When either of these residues is converted to alanine, the mutant shows partial impairment of lipid reorganization. When both are mutated, the protein reorganizes DMPC liposomes similarly to WT. 2) Three independent experimental approaches indicate that Phe^{334} and Trp^{12}/Phe^{15} are in close proximity in the tertiary structure of lipid-free apoA-IV. 3) Systematic disruption of the putative 22-aa amphipathic α-helices provided no evidence that these helices are critical for the initiation of the lipid binding process in apoA-IV. The significance of these findings is discussed below.

Amphipathic α-helices are critical mediators of the reversible lipid binding properties of the exchangeable apolipoproteins (37). It has been proposed that the labile lipid binding of apoA-IV and its rapid displacement from chylomicrons in plasma is due to the relatively hydrophilic nature of its amphipathic α-helices compared with other exchangeable apolipoproteins (38). However, our F334A mutation did not significantly change the overall hydrophobicity and was not located within a putative amphipathic α-helix, yet it caused a dramatic change in lipid association. Thus, the helices of apoA-IV themselves seem to be perfectly capable of rapidly interacting with lipid. The fact that they fail to do this in WT apoA-IV suggests that the lipid binding is attenuated by a conformational effect mediated by the sequence near residues 334 and 335.

Using deletional mutagenesis and spectroscopic techniques, we previously proposed that apoA-IV exists as a large helical bundle composed of residues 40–332. This structure is probably stabilized by the association of the hydrophobic faces of the amphipathic helices. The N- and C-terminal 39 and 44 amino acids, respectively, were not found to be required for the overall stability of this bundle. It is well known that similar helical bundles within apoE and apoA-I open up when structures at the C terminus interact with lipid. This event appears to trigger an extensive conformational change resulting in the sequential binding of each of the helical segments to form an extended lipid-bound conformation and solubilized lipid (39). In apoA-IV, we proposed that the region near residue 334/335 participates in an intramolecular interaction with the N terminus to "lock" the helical bundle in a closed conformation that is unable to rapidly open in the presence of lipid. Our model suggested that disruption of this interaction freed the N-terminal domain, which in turn acted to destabilize the helical bundle. We further speculated that such a destabilization would expose a lipid binding sequence (probably an amphipathic helix) within the

bundle, similar to those of apoA-I and apoE, to trigger lipid binding. Our current work clearly supports the idea that the sequence near residue 334/335 is in close enough proximity to the N terminus of the protein for the proposed interaction. Our FRET studies estimate that residues 12 and 336 are within about 17 Å. The disulfide linkage evident in the double Cys mutant and verified by MS/MS sequencing indicates that the side chains of residues 16 and 336 must come within the minimal distance of 2.3 Å (33). Finally, the BS^3 cross-linking experiment with WT protein puts the extreme N terminus within about 12 Å of residue 339. Based on the hydrophobicity of the amino acids involved, Trp^{12}, Phe^{15}, Phe^{334}, and Phe^{335}, it is tempting to speculate a direct hydrophobic interaction between these residues, perhaps pi-pi stacking. However, it is possible that other residues in the N terminus could be involved.

Although the presence of a C- to N-terminal interaction is strongly supported, the role of the N-terminal residues in mediating lipid binding is less clear. Our initial model suggested that the N-terminal domain, now identified as residues 12 and 15, mediated a destabilizing effect on the helical bundle. However, if this were true, then we might have expected to see a change in apoA-IV conformation when the F334A mutation was present. However, the CD and ANS binding data in Figs. 4 and 5 show that the F334A mutation did not change the overall helicity or the extent of exposed hydrophobic surface area. This suggests that the bundle does not spring open (or even partially open) upon disruption of the N- to C-terminal interaction. In addition, we also expected to see some evidence that one of the amphipathic helical domains within apoA-IV might be an initial lipid binding site comparable with helix 10 in apoA-I. However, Fig. 9 shows that disruption of these helices did not affect the lipid reorganization ability of the F334A mutant. Mutations in one helix appeared to have a modest inhibitory effect, but this was small compared with the effect of similar mutations made in the key lipid binding helix of apoA-I. In light of this, it is plausible that residues 12 and 15 may participate directly in lipid binding and may even comprise the initial trigger for lipid binding. In this revised model, the N-terminal to Phe^{334} interaction may not necessarily hold the bundle closed, but may sequester residues 12 and 15, preventing them from contacting lipid, triggering the opening of the bundle and the subsequent interaction of the amphipathic helical segments with the lipid. This model is dramatically different from those describing apoE and apoA-I lipid binding events.

Intriguingly, the deletion of the N terminus containing Trp^{12} and Phe^{15} from the WT protein without mutating Phe^{334} results in a mutant that reorganizes lipid at the same rate as the WT protein. In fact, we have never found a mutant that is slower than the WT protein. Even the disulfide-linked cysteine mutant seems to clear the solution at about the same rate as WT (Fig. 5). This may indicate that the WT apoA-IV exhibits a minimum basal or perhaps nonspecific clearance that occurs through a different mechanism than the mutants that contain unfettered Trp^{12} and Phe^{15}.

One surprising outcome of the current studies was the fact that the Phe^{334} mutant showed a striking difference from WT apoA-IV in the DMPC clearance assay but was only moderately more efficient in binding the POPC SUV. The DMPC assay measures the end point of a complex process that includes lipid binding and a separate lipid bilayer reorganization step. On the other hand, apoA-IV simply binds to the POPC SUVs without reorganizing them, probably because of the absence of lattice defects that are present in DMPC MLVs at its transition temperature. Our data may indicate that the intramolecular interaction described above is more critical for interaction with lattice defects or the lipid solubilization step than for the interaction of apoA-IV with a static lipid surface. This may have implications for the role of apoA-IV in initial triglyceride-rich lipoprotein assembly when lipids are rapidly being incorporated into the growing particle.

The biological purpose of the attenuation of apoA-IV lipid binding is not yet clear. One possibility is that this acts as a switch mechanism to toggle the lipid reorganization capacity of apoA-IV on or off. There is no published evidence of proteolytic processing of apoA-IV in a way that might perturb the interaction. However, it may be possible for a protein binding event to accomplish this. Interestingly, there is a unique EQQQ repeat between residues 354 and 369 just downstream from Phe^{334}. Perhaps an unknown protein could act as a binding partner for apoA-IV at this location to disrupt the N- to C-terminal interaction, thereby modulating apoA-IV lipid binding characteristics. This control could be important during triglyceride-rich lipoprotein production or may allow apoA-IV to perform functions not shared with other apolipoproteins (*e.g.* a satiety factor role). Using the structural knowledge we have developed, it is now possible to produce apoA-IV mutants that have lipid association "turned on" all the time as well as ones that are perpetually "turned off." These will be useful tools in cell culture models of triglyceride-rich lipoprotein production as well as in engineered mouse studies to determine the significance of this interaction and the role of apoA-IV lipid binding *in vivo*.

Acknowledgment—We thank Dr. Apryll Stalcup for use of the spectropolarimeter for CD measurements.

REFERENCES

1. Green, P. H., Glickman, R. M., Riley, J. W., and Quinet, E. (1980) *J. Clin. Invest.* **65,** 911–919
2. Kalogeris, T. J., Rodriguez, M. D., and Tso, P. (1997) *J. Nutrition* **127,** 537S–543S
3. Weinstock, P. H., Bisgaier, C. L., Hayek, T., Aalto-Setala, K., Sehayek, E., Wu, L., Sheiffele, P., Merkel, M., Essenburg, A. D., and Breslow, J. L. (1997) *J. Lipid Res.* **38,** 1782–1794
4. Gallagher, J. W., Weinberg, R. B., and Shelness, G. S. (2004) *J. Lipid Res.* **45,** 1826–1834
5. Lu, S., Yao, Y., Cheng, X., Mitchell, S., Leng, S., Meng, S., Gallagher, J. W., Shelness, G. S., Morris, G. S., Mahan, J., Frase, S., Mansbach, C. M., Weinberg, R. B., and Black, D. D. (2006) *J. Biol. Chem.* **281,** 3473–3483
6. Ostos, M. A., Lopez-Miranda, J., Marin, C., Castro, P., Gomez, P., Paz, E., Jimenez Pereperez, J. A., Ordovas, J. M., and Perez-Jimenez, F. (2000) *Atherosclerosis* **153,** 209–217
7. Duverger, N., Tremp, G., Caillaud, J. M., Emmanuel, F., Castro, G., Fruchart, J. C., Steinmetz, A., and Denefle, P. (1996) *Science* **273,** 966–968
8. Cohen, R. D., Castellani, L. W., Qiao, J. H., Van Lenten, B. J., Lusis, A. J., and Reue, K. (1997) *J. Clin. Invest.* **99,** 1906–1916
9. Ostos, M. A., Conconi, M., Vergnes, L., Baroukh, N., Ribalta, J., Girona, J.,

Caillaud, J. M., Ochoa, A., and Zakin, M. M. (2001) *Arterioscler. Thromb. Vasc. Biol.* **21,** 1023–1028
10. Kronenberg, F., Stuhlinger, M., Trenkwalder, E., Geethanjali, F. S., Pachinger, O., von Eckardstein, A., and Dieplinger, H. (2000) *J. Am. Coll. Cardiol.* **36,** 751–757
11. Ezeh, B., Haiman, M., Alber, H. F., Kunz, B., Paulweber, B., Lingenhel, A., Kraft, H. G., Weidinger, F., Pachinger, O., Dieplinger, H., and Kronenberg, F. (2003) *J. Lipid Res.* **44,** 1523–1529
12. Kronenberg, F., Kuen, E., Ritz, E., Konig, P., Kraatz, G., Lhotta, K., Mann, J. F. E., Muller, G. A., Neyer, U., Riegel, W., Riegler, P., Schwenger, V., and von Eckardstein, A. (2002) *J. Am. Soc. Nephrol.* **13,** 461–469
13. Warner, M. M., Guo, J. X., and Zhao, Y. M. (2001) *Chin. Med. J.* (*Engl.*) **114,** 275–279
14. Palgunachari, M. N., Mishra, V. K., Lund-Katz, S., Phillips, M. C., Adeyeye, S. O., Alluri, S., Anantharamaiah, G. M., and Segrest, J. P. (1996) *Arterioscler. Thromb. Vasc. Biol.* **16,** 328–338
15. Panagotopulos, S. E., Witting, S. R., Horace, E. M., Hui, D. Y., Maiorano, J. N., and Davidson, W. S. (2002) *J. Biol. Chem.* **277,** 39477–39484
16. Lagrost, L., Gambert, P., Boquillon, M., and Lallemant, C. (1989) *J. Lipid Res.* **30,** 1525–1534
17. Dieplinger, H., Lobentanz, E. M., Konig, P., Graf, H., Sandholzer, C., Matthys, E., Rosseneu, M., and Utermann, G. (1992) *Eur. J. Clin. Invest.* **22,** 166–174
18. Pearson, K., Saito, H., Woods, S. C., Lund-Katz, S., Tso, P., Phillips, M. C., and Davidson, W. S. (2004) *Biochemistry* **43,** 10719–10729
19. Pearson, K., Tubb, M. R., Tanaka, M., Zhang, X. Q., Tso, P., Weinberg, R. B., and Davidson, W. S. (2005) *J. Biol. Chem.* **280,** 38576–38582
20. Lohse, P., Kindt, M. R., Rader, D. J., and Brewer, H. B., Jr. (1991) *J. Biol. Chem.* **266,** 13513–13518
21. Segrest, J. P., Jones, M. K., De Loof, H., Brouillette, C. G., Venkatachalapathi, Y. V., and Anantharamaiah, G. M. (1992) *J. Lipid Res.* **33,** 141–166
22. Markwell, M. A., Haas, S. M., Bieber, L. L., and Tolbert, N. E. (1978) *Anal. Biochem.* **87,** 206–210
23. Pownall, H. J., Massey, J. B., Kusserow, S. K., and Gotto, A. M., Jr. (1978) *Biochemistry* **17,** 1183–1188
24. Segall, M. L., Dhanasekaran, P., Baldwin, F., Anantharamaiah, G. M., Weisgraber, K. H., Phillips, M. C., and Lund-Katz, S. (2002) *J. Lipid Res.* **43,** 1688–1700
25. Davidson, W. S., Ghering, A. B., Beish, L., Tubb, M. R., Hui, D. Y., and Pearson, K. (2006) *J. Lipid Res.* **47,** 440–449
26. Slavik, J. (1982) *Biochim. Biophys. Acta* **694,** 1–25
27. Woody, R. W. (1995) *Methods Enzymol.* **246,** 34–71
28. Chen, Y. H., Yang, J. T., and Martinez, H. M. (1972) *Biochemistry* **11,** 4120–4131
29. Alley, S. C., Shier, V. K., Abel-Santos, E., Sexton, D. J., Soumillion, P., and Benkovic, S. J. (1999) *Biochemistry* **38,** 7696–7709
30. Trakselis, M. A., Alley, S. C., Abel-Santos, E., and Benkovic, S. J. (2001) *Proc. Natl. Acad. Sci. U. S. A.* **98,** 8368–8375
31. Silva, R. A., Hilliard, G. M., Fang, J., Macha, S., and Davidson, W. S. (2005) *Biochemistry* **44,** 2759–2769
32. Silva, R. A., Schneeweis, L. A., Krishnan, S. C., Zhang, X., Axelsen, P. H., and Davidson, W. S. (2007) *J. Biol. Chem.* **282,** 9713–9721
33. Bhattacharyya, R., Pal, D., and Chakrabarti, P. (2004) *Protein Eng. Des. Sel.* **17,** 795–808
34. Weinberg, R. B. (1988) *Biochemistry* **27,** 1515–1521
35. Lu, B., Morrow, J. A., and Weisgraber, K. H. (2000) *J. Biol. Chem.* **275,** 20775–20781
36. Sahoo, D., Weers, P. M. M., Ryan, R. O., and Narayanaswami, V. (2002) *J. Mol. Biol.* **321,** 201–214
37. Brouillette, C. G., and Anantharamaiah, G. M. (1995) *Biochim. Biophys. Acta* **1256,** 103–129
38. Weinberg, R. B., and Spector, M. S. (1985) *J. Lipid Res.* **26,** 26–37
39. Tanaka, M., Dhanasekaran, P., Nguyen, D., Ohta, S., Lund-Katz, S., Phillips, M. C., and Saito, H. (2006) *Biochemistry* **45,** 10351–10358